RSC Advances

ROYAL SOCIETY OF CHEMISTRY

www.rsc.org/advances

Ultra-sensitive Detection of Heparin Via aPTT Using Plastic Antibodies on QCM-D Platform

Munawar Hussain*

Biosensor Research Group, Institute of Clinical and Experimental Transfusion Medicine and Centre of Clinical Transfusion Medicine (ZKT), Tuebingen University and German Red Cross Blood Transfusion Service BW/H, Germany, Correspondence should be addressed to M.H. (munawar_arif@hotmail.com)

One of the challenges faced by todays' clinics is unavailability of practical, precise and accurate determination of the most commonly used anti-coagulant 'heparin' in human blood/plasma in surgery. This is the first report for application of heparin imprinted thin film on Quartz Crystal Microbalance with Dissipation (QCM-D) platform. Based on a novel, straight-forward and robust imprinting approach, a lowest volume consumption of 2 µL of real sample (of human plasma) has been demonstrated. This is a leap step for launching spot test for heparin sensing in laboratory practice. This approach could shorten the coagulation times to 48% and 45% for clinically important sensing range of heparin doses of 0.75 and 0.50 IU/mL respectively and could improve precision to 3 times (n=20 samples) on comparing to that of today's 'gold standard'. Activated partial thromboplastin time (aPTT) on plastic antibodies based QCM-D platform for plasma with doses of heparin 0.75 IU/mL and 0.50 IU/mL yielded 6.5% and 5% lower %RSD respectively as compared to that of 'gold standard'. Present studies could provide a launching pad to laboratory method for ultra-refining of point of care (POC) settings in the perspectives of coagulation time shortening, precision of method and sample volume consumption.

Key Words: Supramolecular Imprinting, Heparin, Plasma, aPTT, Fibrinogen, QCM-D

INTRODUCTION

Molecularly imprinted polymers ((MIPs) i.e. plastic antibodies)) have been demonstrated for detection of proteins [1,2], drugs [3] and pharmaceuticals [4] for clinical [5] and biological [6] applications[7]. MIP technology could be interesting in laboratory and clinics by employing straightforward, simple and selective approaches for challenging detection of supra-molecules (largest templates) in complex medium of human blood/plasma. Supramolecular imprinting is a key for bio sensor applications[8,9,10,11,12].

One of the challenges faced by todays' clinics is unavailability of precise and accurate determination of a vital biomolecule and the most commonly used anti-coagulant 'heparin' in human blood/plasma in surgery[13].

Heparin molecule, the most charge-dense naturally occurring polyanion known in biology, is a linear polysaccharide consisting mainly of 1–4 linked uronic acid and glucosamine subunits. Structure of heparin is shown in Figure 1.

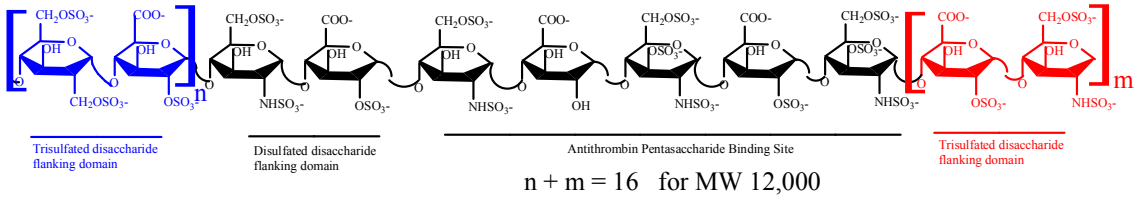

Introduction Figure 1: Heparin structure (poly disperse oligosaccharide-an example).

Sulfation groups in different degrees along disaccharide make heparin the most structurally complex member of the glycosaminoglycan (GAG) class with the polymer Mr spanning ca. 2500–25 000 Da. In all surgical events heparin levels in the blood/plasma are monitored via an activated clotting time assay (best known as aPTT) to ensure the correct amount administration for desired clinical outcome[14]. Astonishingly this area has received an attention from multidisciplinary experts of every fundamental domains of science in the perspectives of laboratory and clinical methods [15,16,17,18,19,20,21,22,23,24].

The primary criteria for POC settings for an anticoagulant monitoring (especially heparin) include convenience, coagulation time shortening, precision, accuracy, lowest sample volume consumption. Other features for such bio sensing include information from single set of measurements, cost-effectiveness, robustness, straightforwardness, quickness, lowest method interferences and improved instrumental miniaturization. For heparin monitoring, 'aPTT' is 'gold standard', universal and inexpensive test on 'standard mechanical coagulometer'. With the lapse of 100 years since first coagulation test, today's research laboratory/clinic still needs trained professional for this area[25].

Heparin results via aPTT are variable for a specific concentration of heparin in different human blood/plasma samples. Heparin monitoring at lower concentration levels is still a chellange[13]. To target this challenge, a straightforward and robust surface imprinting approach using affine pathways has been demonstrated in **figure 2**.

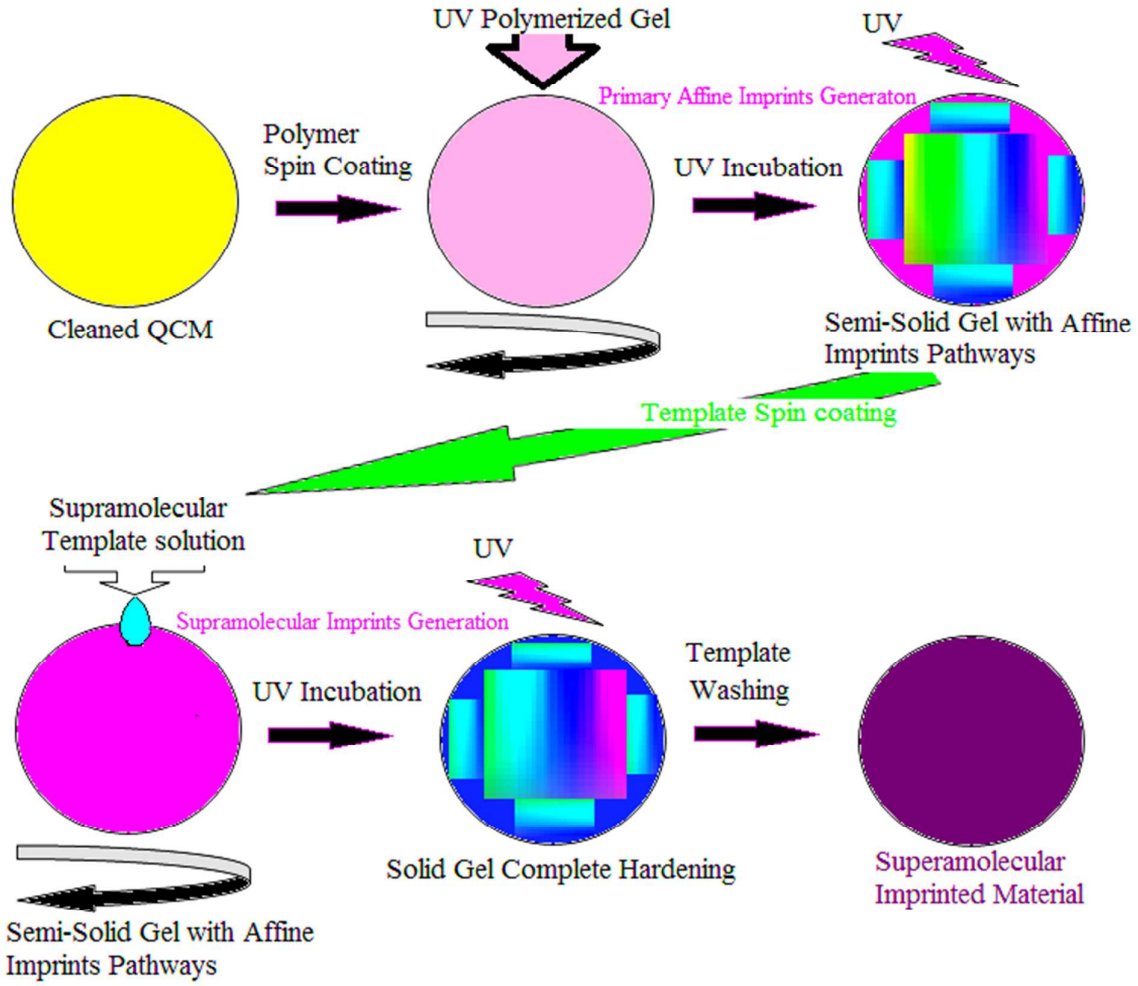

Figure 2: Supramolecular imprinting using affine imprints pathways

In the first step, primary affine imprints have been achieved in a semi solid gel via photo polymerization. In the second step, supramolecular template solution (heparin) was spin coated at extremely fast speed onto nascent primary imprinted gel to achieve surface imprinting under UV. In the end, template was washed to get surface imprinted thin film of main skeleton of heparin.

Continuing previous studies[26,27] on haemostasis and applying novel surface imprinting approach on novel QCM-D (namely qCell T) lowest historical volume of 2 µL of human plasma for POC for aPTT has been demonstrated. MIP based QCM-D using the lowest sample volume 2 µL is cost effective in comparison with standard method that uses 50 folds

(i.e. 100 µL) sample volume consumption for laboratory experiments. Furthermore, QCM is known for its robustness, straightforwardness and cost-effectiveness for bio sensing applications as compared to its counterparts[28]. This is the first report for application of heparin imprinted thin film on QCM-D platform[29]. This approach could shorten coagulation time (aPTT) to 48%±2% and 45%±2% for clinically important heparin sensing range 0.75 and 0.50 IU/mL respectively and could yield 3 times précised data (for n=20 samples) on comparing with today's clinical 'gold standard's'. This could resolve the clinical challenge of highly variability of aPTT in the perspectives of precision and accuracy for a specific concentration of heparin in different human blood/plasma samples. These findings could provide a proof of principle for MIP-based QCM-D application for anticoagulant monitoring and ultra-refining of POC for laboratory method.

EXPERIMENTAL

Chemicals and Reagents: N-methyl pyrrolidone, 1-Vinyl-2-pyrrolidone (VP), Di vinyl benzene (DVB), acetone, dimethylformamid (DMF), danaparoid Sodium and a,a'-azobisisobutyronitrile (AIBN) with highest purity were purchased from Sigma-Aldrich. Sodium chloride (VWR International BVBA) and Tris (2-hydroxy ethyl) amine hydrochloride (TRIS) (PAESEL+LORI GMBH & CO) were used to prepare 50 mM TRIS buffer pH 7.4. Heparin-Natrium-25000- (Ratiopharm) doses were made in 50 mM TRIS buffer (pH 7.4). Citrate solution (0.106 mol l^{-1}(10,0 ml)) and aPTT Coagulation activator Dade Actin® FS were purchased from 9NC S-Monovette and Siemens Health care/Dade Behring, Germany respectively.

Equipment/Instrument: Spin-coater (Spin150-v3, Semiconductor Production Systems, Germany), Centrifuge (Thermo Scientific, Multifuge 3S-R, Kendro Laboratory Products, Germany), UVACUBE 100 (λ_{max} 350 nm, Hönle UV Technology

Germany), "qCell T" (launched in market in 2014, 3T Analytik, Germany), Mechanical coagulometer Merlin MC 1 (Merlin Medical, ABW Medizin und Technik, Lemgo, Germany) and AFM (VEECO Instruments Nanoscope Iva).

Polymer Synthesis: For polymer synthesis; 4 mg AIBN as polymerization initiator was mixed into a mixture of 30 µL VP, 70 µL DVB, 15 µL DMF and 500 µL acetone in the reaction vial. The resulting homogenous solution was kept under UV lamp for 3 hours.

QCMs Cleaning: QCMs were cleaned with N-methyl pyrrolidone and subsequently by acetone.

MIP/NIP Thin Films Synthesis: The polymer was further diluted with 600 µL acetone. 15 µl of polymer was spin coated at 6000 rpm for 90 seconds onto front electrode of each cleaned QCM to achieve a 10 nm thin film. qCell T was used to control layer height of thin film on each QCM. qCell T works as network-analyzer to detect layer height. The spin coated QCMs were kept under UV for 30 minutes for semi-hardening of the thin films for affine pathways generation from DMF and acetone on poly VP-DVB system. For MIP thin film generation, 10 µL of 1:1 (v/v) (20% heparin: 0.025 mol/l $CaCl_2$) as template was further spin coated at 6000 rpm for 1 minute onto semi hardened gel thin film of each QCM. Then QCMs were kept under UV lamp for 2 hours for complete hardening of MIP thin films. Afterwards, the template molecules were washed with spray of distilled water at 40 °C and dried under stream of nitrogen (or kept in desiccator for storage) prior to coagulation measurements on qCell T. For non-imprinted polymer (NIP) thin films, QCMs were processed in the same way without template spin coating step.

Human Plasma Samples: The donation of human whole blood samples from healthy donors was approved by the local ethical committee of the university hospital of Tuebingen, (Institute for Clinical and Experimental Transfusion Medicine) Germany. The participants provided their written consent to participate in this study. Fresh blood samples from healthy donors

were gathered in syringes containing 1.0 ml of 0.106 mol l^{-1} citrate. These samples were centrifuged at 2500 x G for 15 minutes at room temperature and platelets poor plasma (PPP) were separated for measurements.

aPTT Measurements (QCM-D): QCMs having MIP/NIP thin films were mounted on qCell T and were calibrated at 37 °C to achieve stable baseline. Each PPP was induced with 0.0, 0.25, 0.5, 0.75 IU/mL heparin to obtain heparin concentrations. 6 µl of aPTT activator was incubated at 37 °C for one minute in an Eppendorf tube and 6 µl of PPP was mixed. The mixture was re-incubated in the incubation chamber of qCell T at 37 °C for three minutes. By using micropipette, 6 µl of 0.025 mol/l $CaCl_2$ (aPTT starter) at 37 °C was mixed into the incubated mixture and 6 µl from resulting mixture (scientifically speaking having 2 µl of real plasma) was injected immediately into the centre of incubated QCM-D (qCell T). It is important to mention here that injected mixture contains 2 µl of human plasma (PPP) i.e. the shortest volume used in the history of haemostasis to date for aPTT. This is crucial support for POC providing future implementation of automated QCM-D instrumentation for laboratory or clinics. As today's clinical set up relies on disposals to avoid contamination rather than reusable, all aPTT-QCM-D measurements were carried on unused/new thin films and used QCMs were disposed immediately into wastage to avoid contamination[7].

aPTT Measurements (Standard Mechanical Coagulometer): For comparative aPTT measurements, all PPP probes were subjected to mechanical coagulometer measurements at the same time in parallel to qCell T by using100 µl volumes with equal mixing ratios and incubation times.

Scanning electron microscopy (SEM): MIP/NIP thin films on the QCM were visualized by SEM. QCMs were critical point dried (CPD), sputtered with gold palladium, and visualized by using SEM.

AFM (Atomic force microscopy): MIP/NIP thin films on QCMs were also visualized by using contact mode with silicon nitride tip.

RESULTS AND DISCUSSION

By applying rigid ultrasensitive MIP thin film at nm levels on QCM transducer could lead to a frequency shift according to the Sauerbrey equation[30]. Additional viscosity or density shifts of wetting liquids or mass shifts e.g. from cells or bio-films are determined by the Kanazawa equation[31,32].

SEM and AFM images for MIP and NIP demonstrated flat surface morphology. SEM and AFM images of MIP have been shown in **figure 3A and 3B** respectively.

Figure 3

The surface morphology for both cases of MIP and NIP with outstanding homogeneous layout is suitable for coagulation measurements. After surface morphological study, the QCM transducers containing MIP thin films were applied to aPTT coagulation measurements by employing sensor platform as demonstrated in experimental section. Exemplary measurements of aPTT for human real plasma coagulation along with negative controls on MIP have been demonstrated in **Figure 4A.**

The purpose of application of MIP for plasma (without heparin) was to investigate into the imprinted thin film for routine aPTT, total coagulation and fibrinogen sensing in real plasma samples without anticoagulant. Both frequency (Δf (Hz)) and (ΔΓ (Hz) (damping) curves demonstrate outstanding differentiation of coagulation on comparing with negative controls. Bandwidth (Δ Γ Hz) and dissipation (*D)* are essentially the same and are related according to following equation.

$\Delta \Gamma\ (\mathrm{Hz}) = 2D/fn$

fn is the QCM resonance frequency at overtone *n.*

Merging aPTT measurements with those of negative control measurements (i.e. without coagulation), differentiation of the coagulation signals from counterparts in the perspective of shapes/magnitudes of both cases of frequency and dissipation shifts can be done. aPTT coagulation point has been demonstrated as "red star" indicator, this is just the start of falling (down lift) of frequency after stability of frequency curve and is opposite behaviour in dissipation curve, i.e. start of uplift of dissipation after the stability of the dissipation curve. Coagulation process continues after the aPTT coagulation point and ends at the reach of total coagulation that is demonstrated as "black star" indicator in both cases of frequency and dissipation curves respectively. On the other hand, standard coagulometer measures aPTT point during coagulation where the plasma (having coagulation reagent and starter) viscosity exceeds a predetermined viscosity threshold. The aPTT obtained from the MIP or NIP employing QCM-D (tMIP-QCM) or (tNIP-QCM) respectively, can be directly compared with the coagulometer's (tCoag's). The exemplary curves from MIP and NIP on QCM measurements of plasma from one healthy donor having heparin concentrations i.e. 0.25, 0.50, 0.75 IU/mL have been demonstrated in **Figure 4B-4D**. Additional kinetic information of monitoring of total coagulation on QCM-D curves is substantial for POC perspective that makes QCM-D unique;[33] is not possible in standard coagulomerer (as it picks one threshold point during coagulation). This information both on frequency and dissipation curves is substantial to monitor the mass effects from the mass directly attaching to the MIP or NIP surface thin film. Heparin imprinted-MIP on comparing with NIP and standard coagulometer, in principle should shorten the coagulation times (kinetics) depending on heparin levels in the plasma. These characteristics of heparin effect in both cases of frequency and dissipation shifts on MIP and NIP respectively are due to visco-elastic properties of polymeric affinity based on imprinting and non-imprinting respective effects towards heparin concentrations in plasma. Furthermore hydrophobic properties of the thin film play substantial role in real time coagulation kinetics sensing; in the form of aPTT and total coagulation points. aPTT on MIP

for plasma having heparin 0.75 IU/mL is 48% shorter as compared to NIP's; has been demonstrated in **figure 4B.** aPTT on MIP for plasma having heparin 0.50 IU/mL is 45% shorter as compared to NIP's and this has been demonstrated in **figure 4C**. Higher concentration of heparin (0.75 IU/mL) governs efficient heparin molecules penetration into the MIP cavities for holding the plasma clot to the MIP surface, thus kinetically 3% shortening of aPTT point on comparing with that of 0.50 IU/mL. A kinetic shortening of aPTT for precision and accuracy of method at these clinically important doses of heparin is crucial for governing therapeutic directions in surgical room. aPTT on MIP for plasma having 0.25 IU/mL (or lower concentration i.e. 0.00 IU/mL in **Figure 4**) heparin compared to NIP's (**figure 4D)** yielded no difference in kinetics; both MIP and NIP signals are overlapping.

Figure 4

Further investigation into the application of MIP or NIP for more real samples of human plasma is necessary and important because of extremely complex nature of human real blood/plasma[13]. Plots directly comparing tMIP-QCM (or tNIP-QCM) (where "t" means aPTT) of plasma samples (n=20 for each case) having different heparin concentrations with corresponding tCoag are demonstrated in **figure 5A and 5B.** aPTT gathered from MIP and NIP at 0.50 and 0.75 IU/mL heparin concentrations have been compared in **Figure 5A**; here aPTT of different plasma probes (n=20) collected from coagulometer (tCoag) are plotted versus aPTT measured with QCM (tMIP-QCM or tNIP-QCM) respectively. MIP and NIP demonstrate excellent correlation lines passing through the origin with in analytical limits of deviations. aPTT on MIP-QCM-D for plasma having heparin 0.75 IU/mL and 0.50 IU/mL, are always 48% and 45% respectively shorter as compared to standard coagulometer's (or NIP-QCM-D's). aPTT on MIP-QCM-D for plasma having heparin 0.75 IU/mL and 0.50 IU/mL yielded ranges of 100-130 and 45-80 seconds respectively. aPTT on NIP-QCM-D (or Coag) for plasma having heparin 0.75 IU/mL and 0.50 IU/mL yielded ranges of 170-255 and 70-155 seconds respectively. MIP-QCM-D ranges are 3 and 2.5 times précised at 0.75 IU/mL

and 0.50 IU/mL doses of heparin respectively as compared to standard coagulometer's (or NIP-QCM-D's).

Figure 5

aPTT gathered from MIP (which are same for NIP) at 0.00 and 0.25 IU/mL heparin concentrations have been compared in **Figure 5B,** where aPTT of different plasma probes collected from coagulometer (tCoag) are plotted versus aPTT measured with QCM (tMIP-QCM) respectively. An outstanding correlation between the two methods yielded data points with in ±2SD and a linear line passing through the origin. The data in all cases of plasma probes is within analytical deviation limits overlapping ideal correlation line. This is outstanding in the perspective of POC settings for MIP based QCM-D that uses lowest sample volume of 2 µL in comparison with standard method which uses 50 folds sample volume i.e. 100 µL for laboratory experiments. As mentioned above, plasma probes containing heparin doses of 0.75 IU/mL and 0.50 IU/mL are 48% and 45% respectively shorter on MIP comparing to the standard coagulometer's or NIP's; thus MIP-QCM-D yielded superior sensitivity.

Rational to use heparin MIP is to shorten the coagulation times with in same concentrations of heparin in different human plasma samples and to achieve precision and accuracy for POC. In this regard, Bland-Altman plots[34] for plasma probes having heparin 0.00, 0.25, 0.50 and 0.75 IU/mL heparin for tMIP-QCM (or tNIP-QCM) and tCoag are demonstrated in **Figure 6A and 6B** respectively.

Figure 6

The Bland-Altman plot is crucial to compare the agreement of two techniques/methods, not the correlations, and it also yields a visual overview of the techniques/methods compared.

Bland-Altman plot for tMIP-QCM vs tCoag demonstrates data points within ±2SD agreement with a linear line at 0.00 and 0.25 IU/mL heparin concentrations. Plasma probes containing heparin 0.75 IU/mL and 0.50 IU/mL yielded R^2 values of 0.96 and 0.97 respectively; and 48%±2% and 45%±2% shorter aPTT respectively on MIP. On the other hand, a Bland-Altman plot for tNIP-QCM vs tCoag yielded linear line at 0.00 and 0.25 IU/mL heparin concentration levels and data points within ±2SD agreement. Plasma probes containing heparin 0.75 IU/mL and 0.50 IU/mL yielded linear line with in ±5SD. On comparing precisions of two techniques/methods, at 0.75 IU/mL heparin in plasma samples, tMIP-QCM data range (i.e. 100-130 seconds) is 3 times shorter as compared to tCoag's (that is same for tNIP-QCM) (i.e. 170-255 seconds). At 0.50 IU/mL heparin in plasma samples tMIP-QCM data range (i.e. 45-80 seconds) is 2.5 times shorter as compared to tCoag's (that is same for tNIP-QCM) (i.e. 70-155 seconds). To shrink the silky thread of discussion, MIP based QCM-D data demonstrates outstanding and promising in the perspectives of precision and accuracy for challenging heparin sensing in laboratory/clinics.

A further part of the puzzle is the %RSD data of MIP for heparin in comparison to that of NIP (or standard coagulomer). It has been shown in **Figure 7.** aPTT on MIP-QCM-D for plasma having heparin 0.75 IU/mL yielded %RSD of 8.81, while NIP-QCM-D (or Coag) yielded %RSD of 15.16. aPTT on MIP-QCM-D for plasma having heparin 0.50 IU/mL yielded %RSD of 23.75, while NIP-QCM-D (or Coag) yielded %RSD of 28.34 respectively. The %RSD data of MIP has lower variability as compared to NIP (or Coag).

Figure 7

QCMs are unique sophisticated traditional rheometry and thromboelastometry providing viscoelasticity[35,36] and mass sensitivity. Mass and viscoelastic sensing of the haemostasis at non-molecular scales are the most substantial measures for fibrin polymerization in coagulation, platelets fibrinogen interactions and fibrinolytic processes. Proper love/arranged

marriage of sensor thin film on QCM transducer can yield outstanding and miraculous births of information for coping challenging supramolecular sensing in the perspective of precision and accuracy, behaviour and fast kinetics (aPTT and total coagulation points) in challenging complex samples of human plasma. As demonstrated in introduction **figure 2** and experimental section, primary affine imprints from DMF and acetone have been achieved on VP-DVB for generation of semi solid gel via photo polymerization. Supramolecular template solution (heparin) was spin coated at extremely fast speed of 6000 rpm onto nascent primary imprinted gel having affine pathways to achieve surface imprinting under UV in the second step. Affine pathways generated from C=O (from DMF and acetone) and poly VP-DVB system lead to effective surface imprinting of main skeleton of heparin i.e. polysaccharides groups and C=O groups under photo polymerization. MIPs keep inherent faster kinetics and binding over NIPs[37]. After achieving completely hardened gel and template washing step, the surface imprinted cavities from heparin ultimately lead to fast kinetics, highly sensitive and accurate. MIP over all yielded 48%±2% and 45%±2% shorter aPTT on MIP at 0.75 IU/mL and 0.50 IU/mL heparin respectively in comparison to NIP's (or "gold standard's"). Ultimately MIP yielded 3 and 2.5 times shorter ranges (precision) as compared to NIP's (that is same for tCoag's) at 0.75 IU/mL and 0.50 IU/mL heparin respectively. %RSD data for MIP has lower values. This factor coupled with aPTT shortening on MIP is interesting for POC settings of QCM-D technique. Present study is proof of principles for laboratory research.

CONCLUSIONS

aPTT on MIP-QCM-D for plasma (n=20) with different doses of heparin have been compared to that of NIP-QCM-D (or standard coaglomoeter). aPTT on MIP-QCM-D for plasma having heparin 0.75 IU/mL and 0.50 IU/mL yielded 6.5% and 5% lower %RSD as compared to that of NIP-QCM-D (or standard coaglomoeter) respectively. MIP over all yielded 48%±2% and 45%±2% shorter aPTT on MIP at 0.75 IU/mL and 0.50 IU/mL heparin respectively in

comparison to NIP's (or "gold standard's"). Ultimately MIP yielded 3 and 2.5 times shorter ranges (precision) as compared to NIP's (that is same for tCoag's) at 0.75 IU/mL and 0.50 IU/mL heparin respectively. The MIP-QCM-D for heparin sensing is promising in the perspectives of point of care application in clinical and laboratory applications. Cost-effectiveness, straightforwardness, simple instrumentation and miniaturization of the QCM-D sensor have extraordinary potential for a multi-channel for measuring all haemostasis parameters together with other clinical or laboratory tests simultaneously.

ACKNOWLEDGEMENTS: Oksana Faul is acknowledged for technical assistance in laboratories. Dr. F. K. Gehring and Prof. Dr. H. Northoff are highly acknowledged for discussions and support.

References

1 D. Cai, L. Ren, H. Zhao, C. Xu, L. Zhang, et al., *Nat. Nanotechnol.,* 2010, **5,** 597-601.

2 H. Shi, W. B. Tsai, M. D. Garrison, S. Ferrari, B. D. Ratner, *Nature,* 1999, **398,** 593-597.

3 G. Vlatakis, L. I. Anderson, R. Muller, K. Mosbach, *Nature.* 1993, **361,** 645-647.

4 M. Hussain, N. Iqbal, P. A. Lieberzeit, *Sens. Act. B.* 2013, **21,** 176-186.

5 G. Zheng, F. Patolsky, Y. Cui, W. U. Wang, C. M. Lieber, *Nat. Biotechnol.,* 2005, **23,** 1294-1301.

6 F. Patolsky, G. Zheng, C. M. Lieber, *Nat. Protoc.,* 2006, **1,** 1711-1724.

7 M. Hussain, J. Wackerlig, P. A. Lieberzeit, *Biosensors,* 2013, **3,** 89-107.

8 L. Chen, S. Xuab, J. Li, *Chem. Soc. Rev.* 2011, **40,** 2922-2942.

9 M. J. Whitcombe, *Chem. Soc. Rev.* 2011, **40,** 1547-1571.

10 S. Chaterji, K. Kwon, K. Park, *Prog. Polym. Sci.* 2007, **32(8-9),** 1083-1122.

11 E. Verheyen, J. P. Schillemans, M. van Wijk, M. A. Demeniex, W. E. Hennink, van, C.F. Nostrum, *Biomater.,* 2011, **32,** 3008-3020.

12 R. K. David, A. P. Nicholas, *Acta Biomater.* 2012, **8,** 461-473.

13 M. B. Stephen, E. Wilde, D. K. Smith, *Chem. Soc. Rev.* 2013, **42,** 9184-9195.

14 L. F. John, B. G. James *Pharmacother.* 2004, **24(8-2),** 108S–119S.

15 M. B. Stephen, A. Barnard, P. Posocco, M. Fermeglia, S. Pricl, D. K. Smith, *J.A.C.S.* 2013, **135(8),** 2911-2914.

16 C. R. Ana, B. Anna, C. James, K. S. David, *Angew. Chem. Int. Ed.* 2011, **50,** 4675-4679.

17 Z. Liu, Q. Ma, X. Wang, Z. Lin, H. Zhang, L. Liu, X. Su, *Biosens. Bioelectron*., 2014, **54(15),** 617-622.

18 M. B. Stephen, P. Posocco, M. Fermeglia, S. Pricl, J. R. Lo´pezd, D. K. Smith, *Chem. Commun.,* 2013, **49**, 4830-4832.

19 J. P. Francoia, R. Pascal, L. Vial, *Chem. Commun.,* 2015, **51**, 1953-1956.

20 N. Abramova, A. Bratov, *Electroanalysis.* 2015, **27,** 1-8.

21 M. B. Stephen, P. Posocco, C. W. Chan, M. Calderon, S. E. Guimond, J. E. Turnbull, S. Pricl, D. K. Smith, *Chem. Sci.* 2014, **5**, 1484-1492.

22 L. Hualong, P. Song, R. Wei, K. Li, A. Tong, *Talanta.* 2014, **118(15),** 348-352.

23 M.B. Stephen, P. Posocco, M. Fermeglia, J. Tolosa, A. H. López, S. Pricl, J. R. López D. K. Smith, *Chem. Eur. J.* 2014, **20**, 9666-9674.

24 Z. Jiangna, Y. Yi, N. Mi, B. Yin, M. Wei, Q. Chen, H. Li, Y. Zhang, S. Yao *Talanta,* 2013, **116(15),** 951-957.

25 L. F. Harris, V. C. López, A. J. Killard, *Trend. Anal. Chem.,* 2013, **50,** 85-95.

26 M. Hussain, H. Northoff, F. K. Gehring, *Biosens. Bioelectron*., 2015, **66,** 579-584.

27 M. Hussain, S. Sinn, M. Zeilinger, H. Northoff, P. A. Lieberzeit, F. K. Gehring, *J. Biosens. Bioelectron.,* 2013, **4:4,** 1000139.

28 E. Juzeliūnas, *Chemija.,* 2009, **20 (4),** 218-225.

29 L. Li, Y. Liang, Y. Liu, *Anal. Biochem.* 2013, **434 (2),** 242-246.

30 G. Sauerbrey, *Zeitschrift für Pysik,* 1959, **155,** 206-222.

31 K. K. Kanazawa, J. G. Gordon, *Anal. Chem.,* 1985, **57,** 1770-1771.

32 F. K. Gehring, Schwingquarzsensorik in Flüssigkeiten: Entwicklung eines Blutanalysegerätes. language: DE, Edn. 1, ISBN-13: 9783865378729, Cuvillier Verlag, International Scientific Publisher, Germany 2006, 100**.**

33 D. Breitwieser., et al. *J. Mater. Chem. B.* 2013, **1,** 2022-2030.

34 J. M. Bland, D. G. Altman, *Lancet,* 1986, **1,** 307-310.

35 P. A. Evans, K. Hawkins, M. Lawrence, M. S. Barrow, P. R. Williams, et al. *Clin. Hemorheol. Microcirc.,* **2008,** 38, 267-277.

36 P. A. Evans, K. Hawkins, M. Lawrence, R. L. Williams, M. S. Barrow, et al. *Med. Eng. Phys.,* 2008, **30,** 671-679.

37 H. Surikumaran, S. Mohamad, N. M. Sarih, *Int. J. Mol. Sci.* 2014, **15,** 6111-6136.

Figure 3A

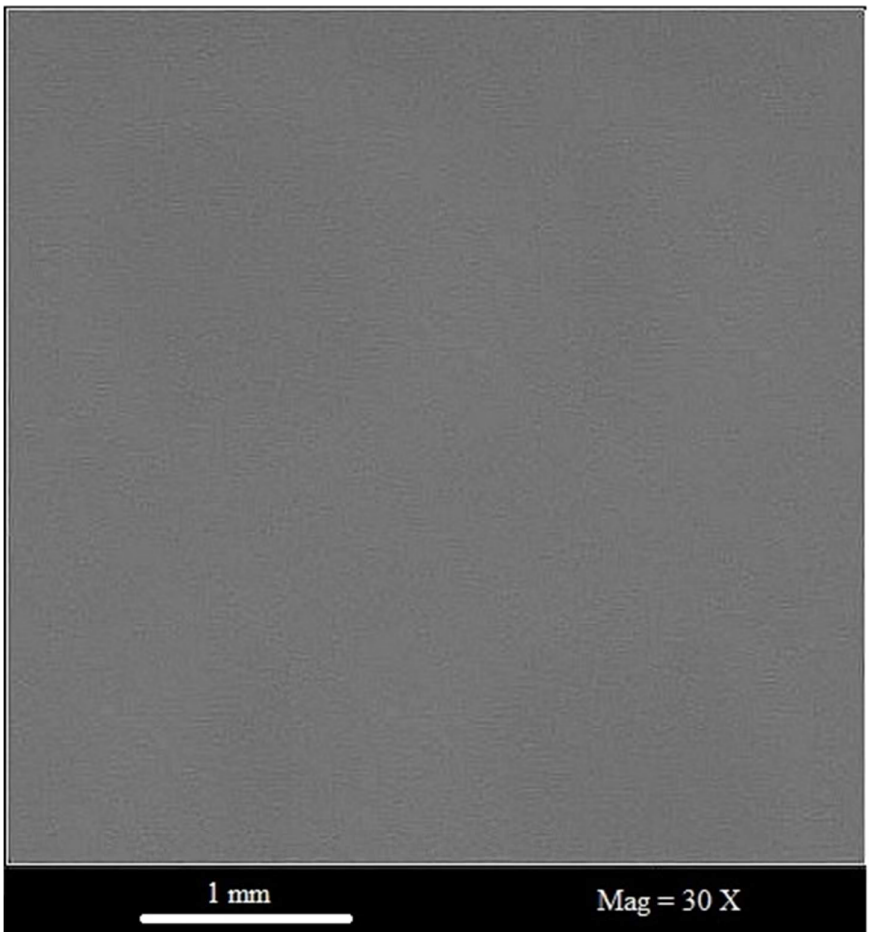

Figure 3A SEM image of Heparin MIP (and similar SEM image for NIP).

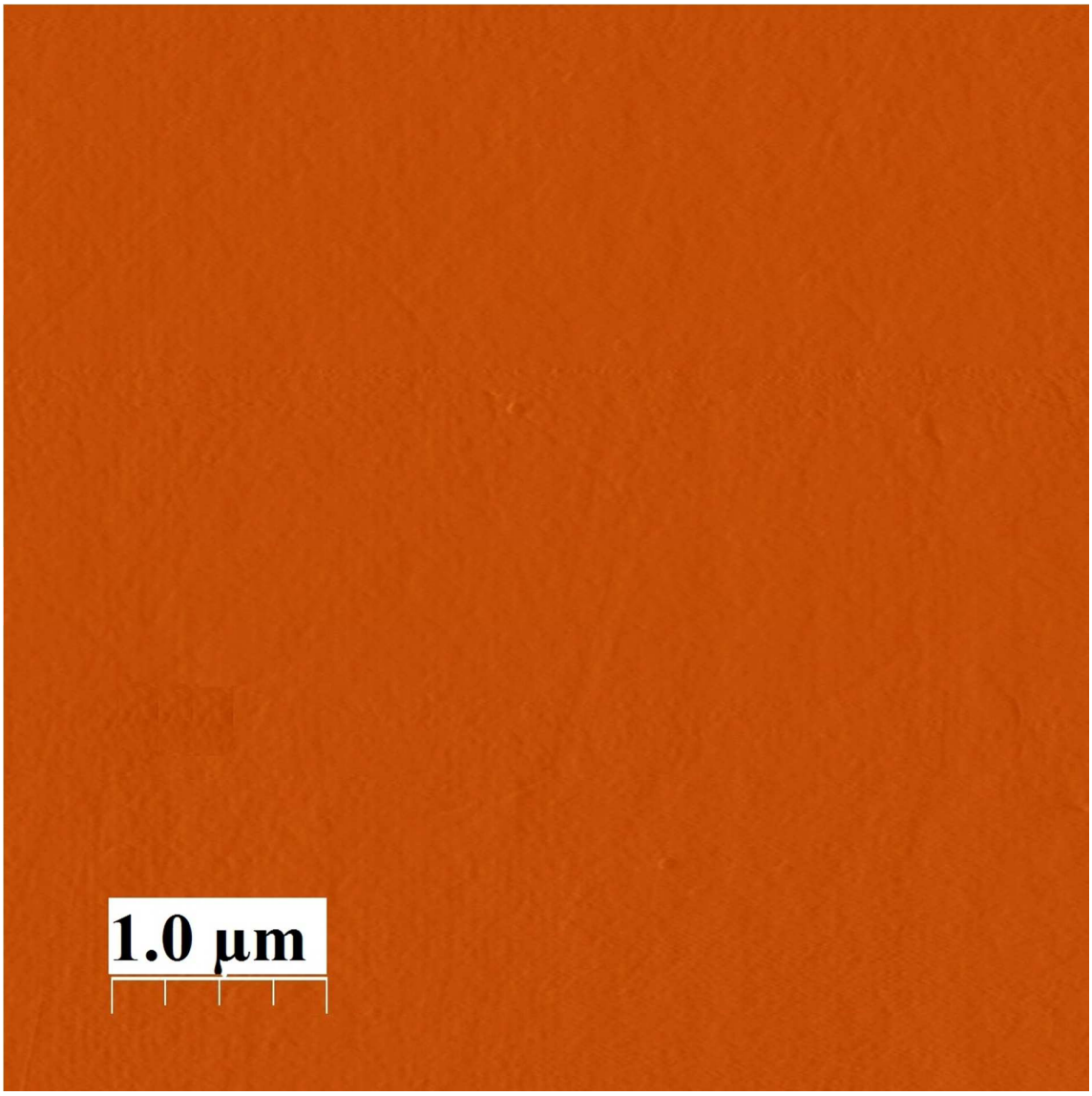

Figure 3B AFM image of Heparin MIP (and similar AFM image for NIP).

Figure 4

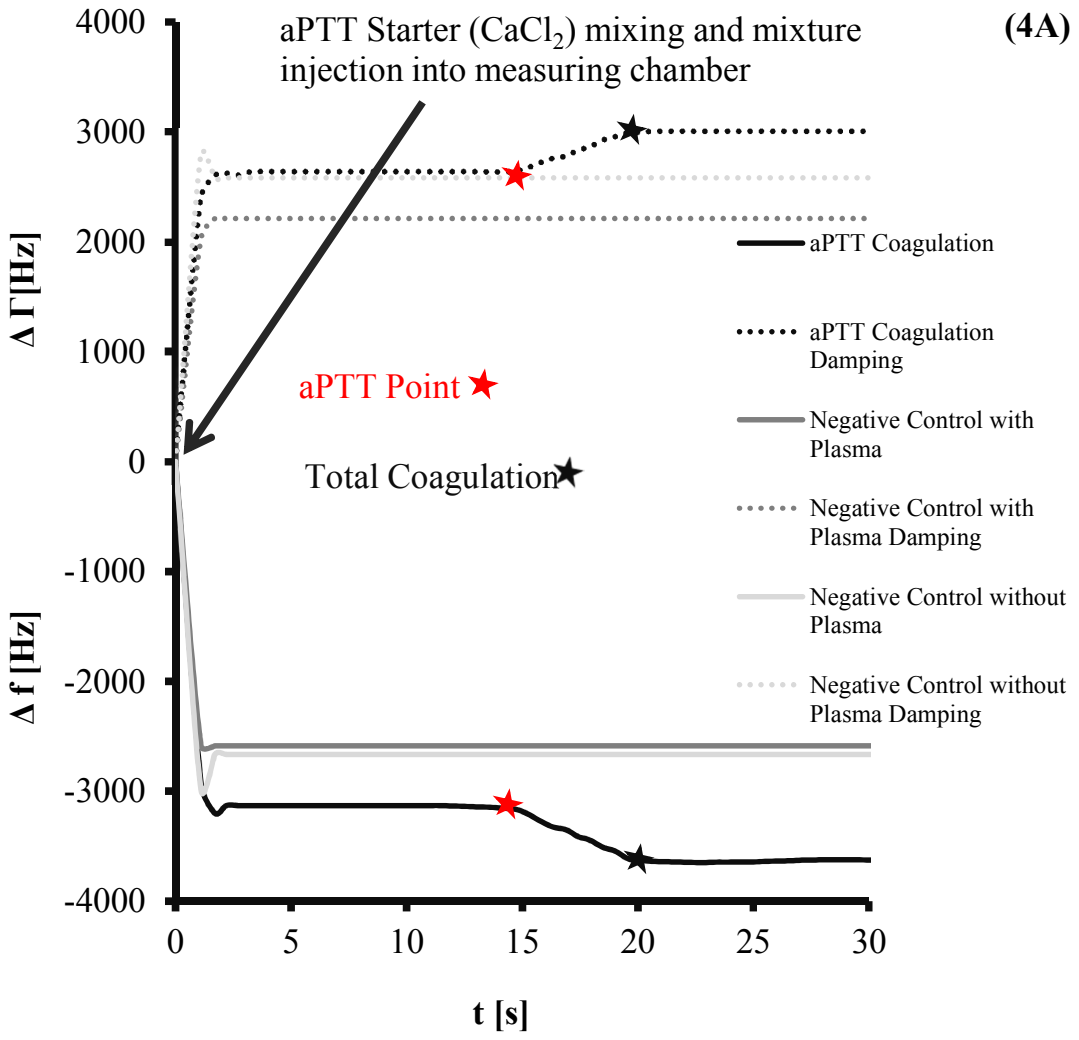

Figure 4A Exemplary measurements of aPTT on MIP-QCM-D for plasma (from a healthy donor) coagulation along with two different negative controls: plasma without coagulation and aPTT-coagulation activator without plasma, aPTT coagulation points and total coagulation points are indicted by red star and black indicators in both cases of frequency and dissipation curves respectively.

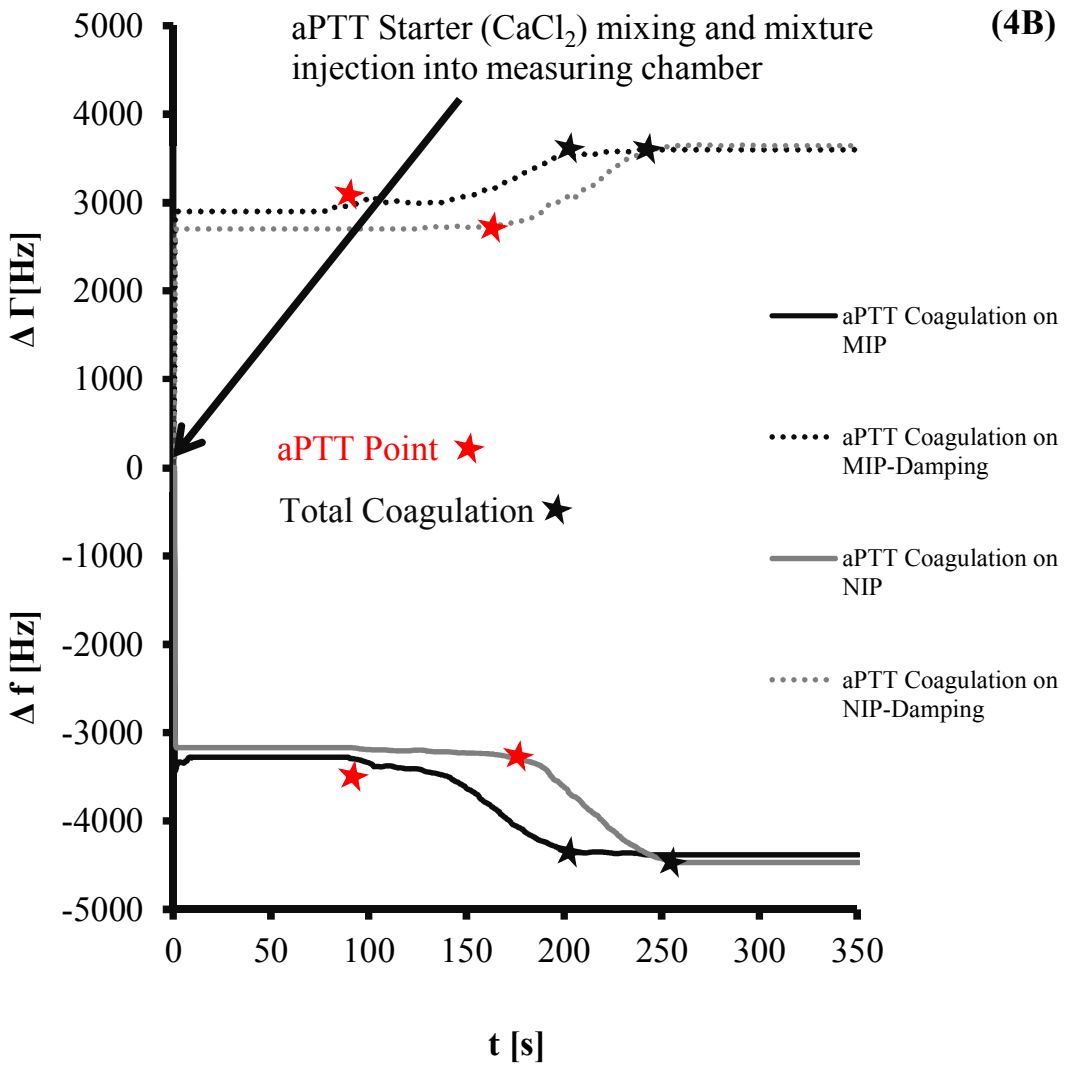

Figure 4B Exemplary measurements of aPTT for plasma (of one healthy donor) coagulation for plasma having heparin 0.75 IU/mL, aPTT-coagulation points are indicted by red and black stars indicators in both cases of frequency and dissipation curves respectively.

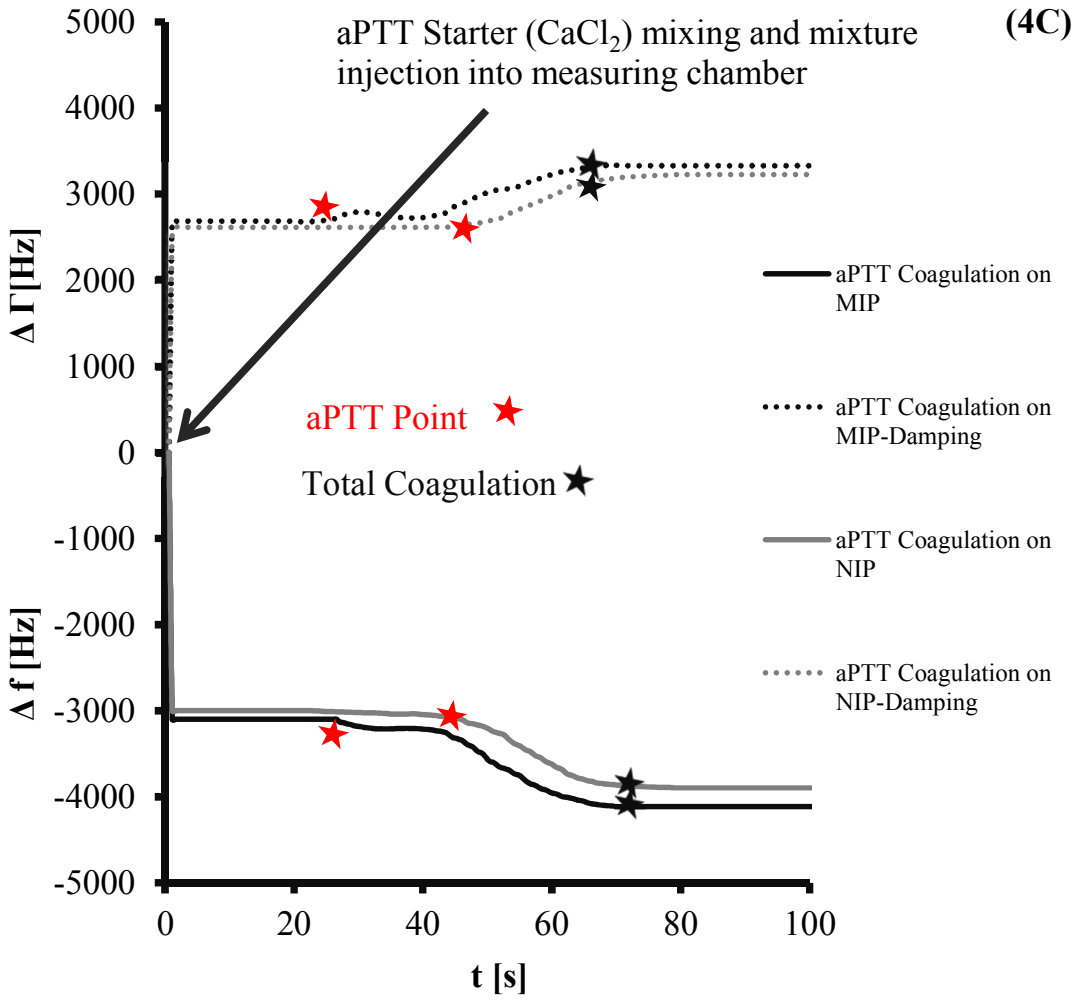

Figure 4C Exemplary measurements of aPTT for plasma (of one healthy donor) coagulation for plasma having heparin 0.50 IU/mL, aPTT-coagulation points are indicted by red and black stars indicators in both cases of frequency and dissipation curves respectively.

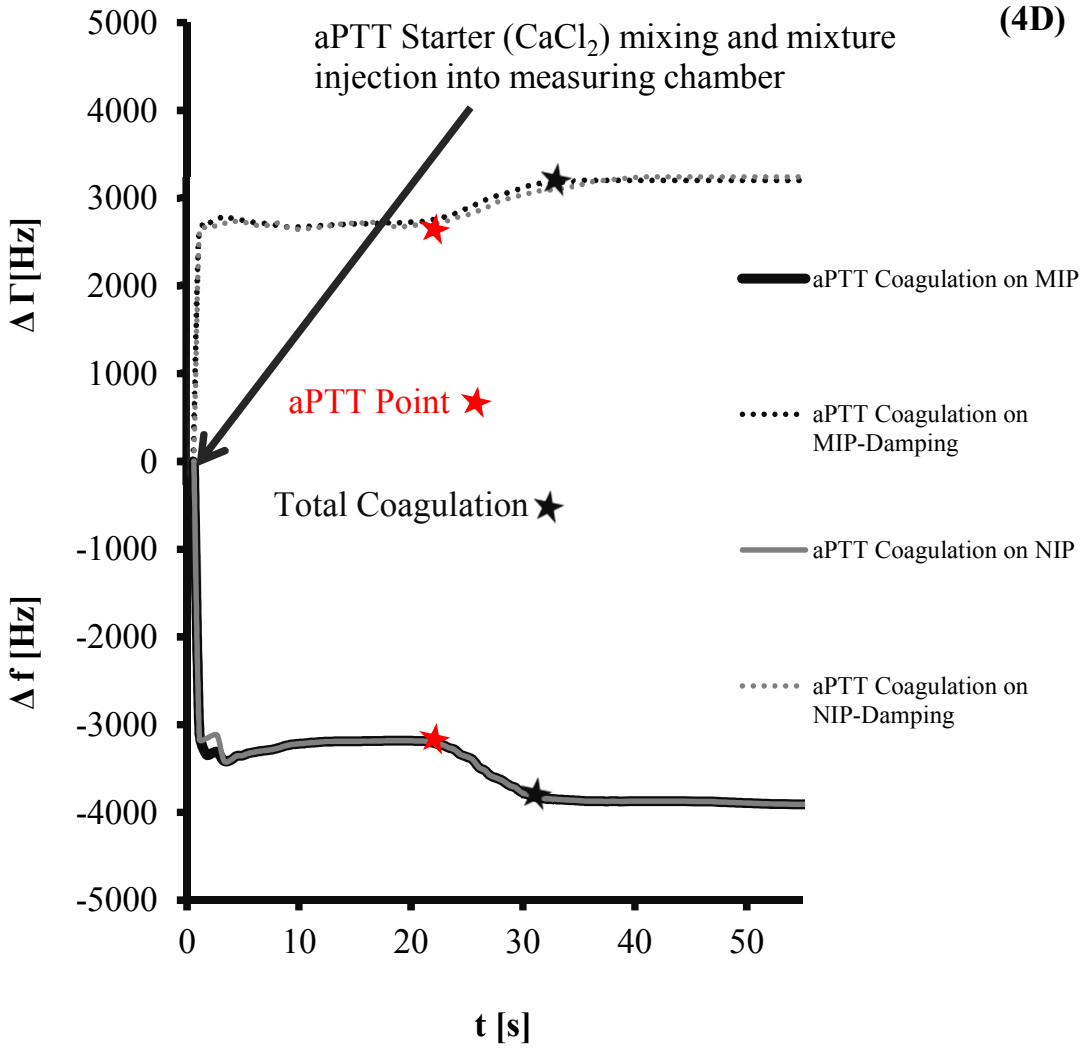

Figure 4D Exemplary measurements of aPTT for plasma (of one healthy donor) coagulation for plasma having heparin 0.25 IU/mL, aPTT-coagulation points are indicted by red and black stars indicators in both cases of frequency and dissipation curves respectively.

Figure 5

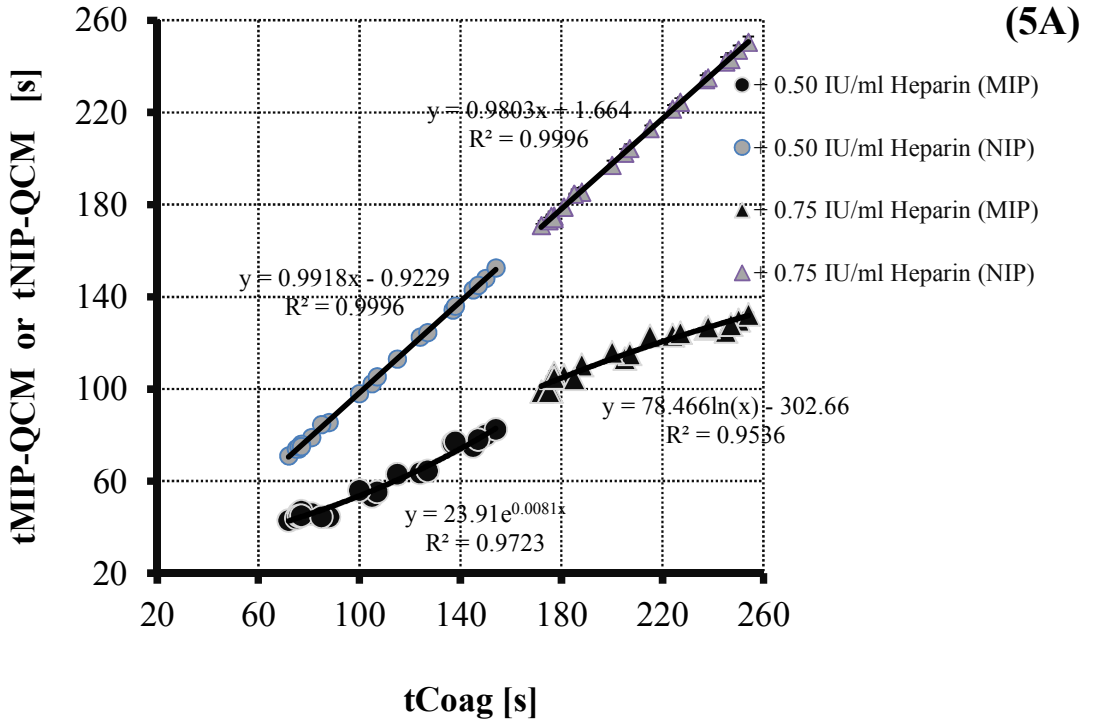

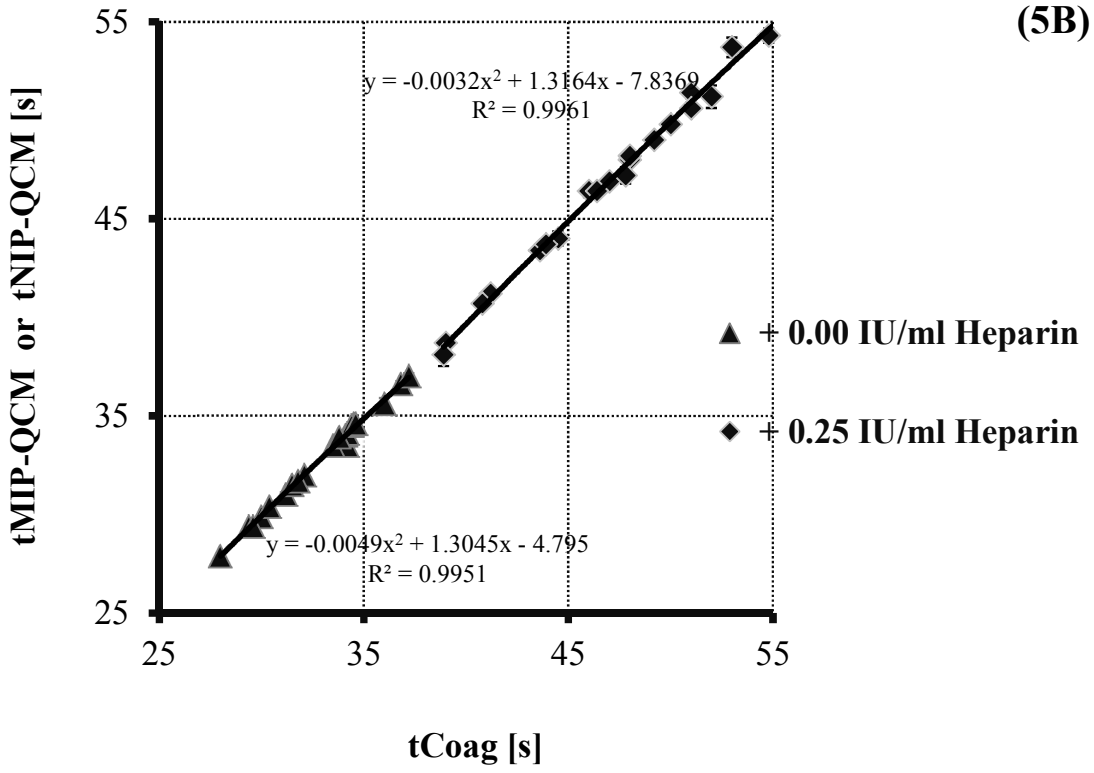

Figure 5 aPTT (i.e. tMIP-QCM-D (or tNIP-QCM-D)) of human plasma obtained from MIP-QCM-D (or NIP-QCM-D) respectively plotted against aPTT (tCoag) obtained with a mechanical coagulometer (gold standard). Plasma samples with different heparin concentrations are given with appropriate symbols. (n=20 plasma samples for each heparin concentration). Each data point demonstrates the mean of three measurements demonstrating error bars ± SD of three measurements.

Figure 6

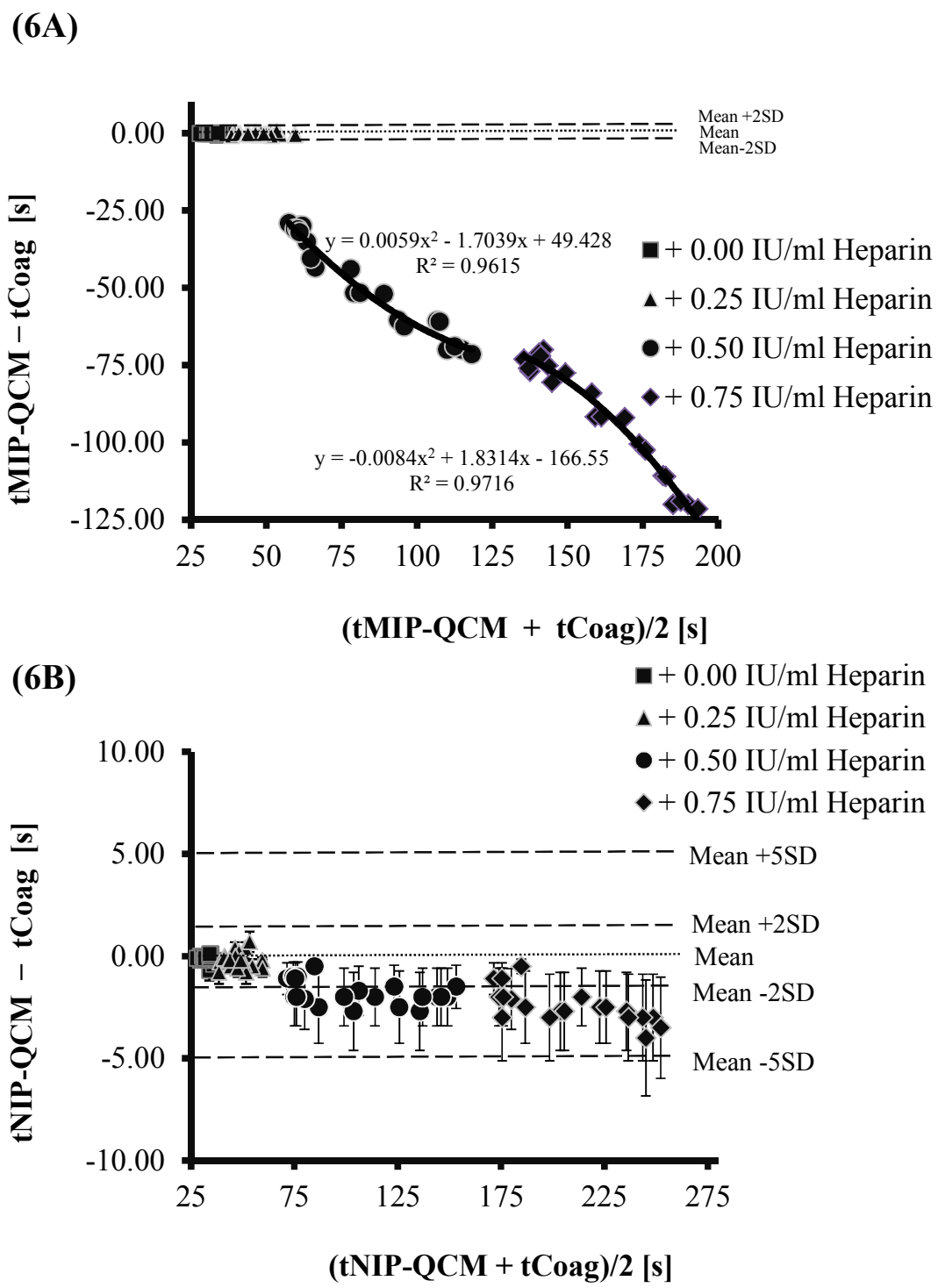

Figure 6 The Bland Altman plot of aPTT measured on MIP-QCM-D (or NIP-QCM-D) and coagulometer, plasma samples with different heparin concentrations are indicated with appropriate symbols (n=20 plasma samples for each heparin concentration).

Figure 7

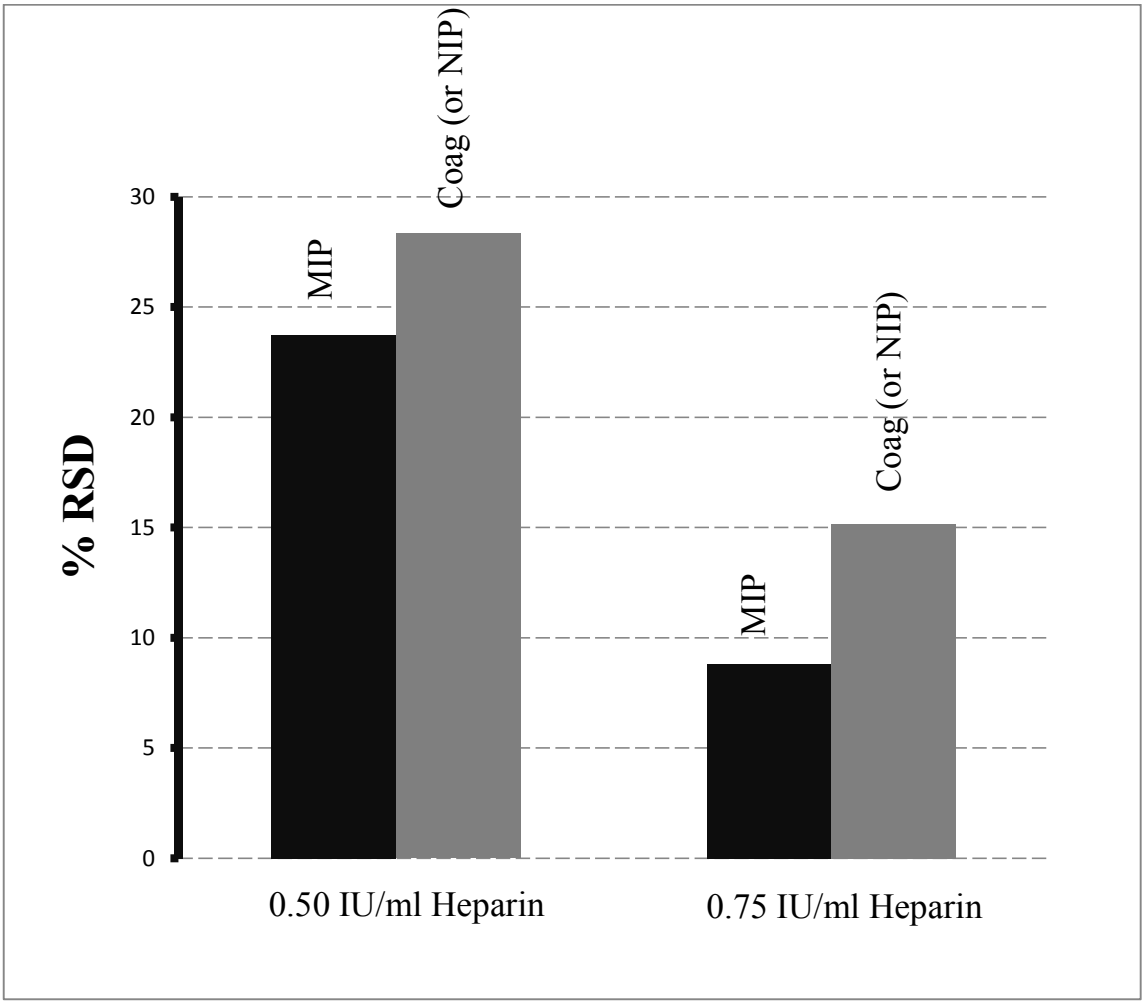

Figure 7 MIP-QCM-D compared with coagulometer (or NIP-QCM-D); %RSD data for plasma of a healthy donors (n=20) induced with heparin doses of 0.75 and 0.50 IU/ml respectively.